Temperature effects on the point defects formation in [111] W by neutron induced collision cascade

F. J. Domínguez-Gutiérrez[1, 2, *]

[1]*NOMATEN Centre of Excellence, National Centre for Nuclear Research,*
ul. A. Sołtana 7, 05-400 Swierk/Otwock, Poland
[2]*Institute for Advanced Computational Science, Stony Brook University, Stony Brook, NY 11749, USA*

Tungsten is used as plasma-facing wall in ITER where it is subjected to extreme operating conditions. In this work, we study the damage formation in [111] crystalline W by neutron bombardment in the temperature range of 300-900 K which is important for designing next generation of fusion reactors. The Molecular Dynamics (MD) simulations are performed at a primary knock-on atoms (PKA) energy of 1 keV within the Gaussian Approximation Potential (GAP) framework. The analysis of the induced damage is done by the Fingerprinting and Visualization Analyzer of Defects (FaVAD) which is based on a rotation invariant mapping of the local atomic neighborhoods allowing to extract, to identify and to visualize the atomic defect formation dynamically during and after the collision cascades. The evaluation allows to classify the various defect types and to quantify the defect evolution as function of time and initial sample temperature. We found that the production of Frenkel pair increases as a function of the temperature due to thermal activated mechanisms.

I. INTRODUCTION

Tungsten is considered as a Plasma Facing Material (PFM) due to its physical and chemical properties such as low erosion rates, small tritium retention, and high melting point which is important to design the next generation of fusion machines. Mechanical properties of W can be enhanced or modified due to irradiation where formed permanent point or extended defects (dislocations) can increase the hardness of the material [1–3]. For this reason, experimental exploration of the characterization of PFMs needs to be guided by numerical modeling saving laboratory and financial resources for carrying out experiments at extreme environments [4–7], where atomistic simulations method can be performed [8–12].

In order to model the formation of point defects due to neutron bombardment, the Molecular dynamics (MD) method is applied to perform simulations of collision cascades. The accuracy of the numerical results is highly dependent on the interatomic potentials capable to describe induced damage in materials [13]. However, traditional potentials based on the embedded atom model (EAM) are limited to functional forms [14, 15] and are in risk to wrongly model some point defects lacking of physical meaning in material damaging processes [16]. Thus, interatomic potentials developed by using machine learning (ML) techniques are recently used to perform MD simulations with an accuracy close to Density Functional Theory (DFT) [12, 17, 18] and systematically improved towards the accuracy of the training data set. In our previous work, we applied interatomic potentials based on the Gaussian Approximation Potential (GAP) framework to numerically model the damage in crystalline materials due to irradiation in a fusion reactor [12, 19]. MD simulations were analyzed by a recently developed workflow

for semi-automatic identification and classification of defects in crystalline structures and reported results are in good agreement with experimental data [20]. Therefore, the goal of the present work is to better understand the thermal activated mechanisms for material damage in crystalline W samples which is commonly used in experiments for irradiation in a fusion reactor. For this, we perform MD simulations to model neutron irradiation in [111] W at 1 keV of PKA in a sample temperature range from 300 to 900 K providing an analysis of the point defects formation after collision cascades.

Our paper is organized as follows: in Section II we briefly discuss the theory to develop the machine learned (ML) potential [12, 21] into the GAP framework, as well as the software workflow for the Fingerprinting and Visualization Analyzer of Defects (FaVAD) [20, 22]. Our results for the total number of points defects and atomic displacement as a function of the sample temperature are presented in Sec. III. Finally, in section IV, we provide concluding remarks.

II. METHODS

MD simulations are traditionally used to model neutron bombardment processes at different PKA energies providing information of damage in crystalline materials. In our work, we start by defining a numerical box with a size of ($81.08\ \hat{x}$, $78.02\ \hat{y}$, $82.75\ \hat{z}$) nm and W atoms arranged into a crystalline body-centered-cubic (BCC) geometry with a lattice constant of $a = 3.18$ Å; according to DFT calculations for computing the GAP potentials [12]. Then, the numerical sample is prepared by a process of energy optimization and thermalization using the Langevin thermostat, with the time constant of 100 fs. [19].

In radiation experiments, the energy of neutrons is around 14 MeV after D+T reaction. Particles can lose

energy through non-ionizing interactions with the materials through displacement damage where the collision energy between incoming particle and a lattice nucleus (Primary Knock-on Atom) is in the order of $10^3 - 10^5$ eV; displacing atoms from original lattice positions to generate point defects. Thus, it has been reported that 1 keV PKA value is at the subcascade energy threshold to produce more than one stable Frenkel pair in crystalline W samples at room temperature [23]. This kinetic energy is assigned to a W atom located at ten different randomly chosen locations with a velocity vector oriented to the center of the sample, as shown in Fig. 1 to mimic damage production at the experimental depths of hundreds of nanometers. The W samples are equilibrated to temperatures of 400, 600, 800, and 900 K to consider conditions into nuclear reactors. The room temperature is used in our work as a reference [15]. Then, the Velocity Verlet integration algorithm is applied to model the collision cascade for 6 ps, followed by an additional relaxation time of 4 ps. The MD simulations were performed in the institutional cluster of the Stony Brook University by using the Large-scale Atomic/Molecular Massively Parallel Simulator (LAMMPS) [24].

A. Gaussian Approximation Potential framework

The Quantum mechanics and Interatomic Potential package (QUIP) [25] is used as an interface to implement machine learned interatomic potentials based on GAP [17] that can be systematically improved by their training data set modifications. The GAP potential mod-
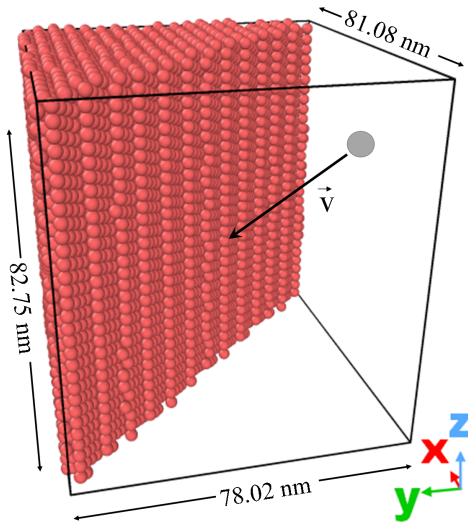

FIG. 1. (Color on-line). Schematic of the prepared numerical box used in the MD simulations with GAP potentials. The sample was sliced on the [-110] × [-1-12] plane for better visualization of the crystal orientation and projectile's initial position into the sample, as well as the orientation of its velocity vector.

els collision cascades mechanisms due to its training data set for describing short-range dynamics, the liquid phase, and the re-crystallization process where defect creation and annihilation tend to happen [12, 16]. Here, the total energy of a system of N atoms is expressed into the GAP framework as

$$E_{\text{tot}} = \sum_{i<j}^{N} V_{\text{pair}}(r_{ij}) + \sum_{i}^{N_d} E_{\text{GAP}}^i, \qquad (1)$$

where V_{pair} is a purely repulsive screened Coulomb potential. The term E_{GAP} is obtained by using the Smooth Overlap of Atomic Positions (SOAP) package [17] with N_d as the number of descriptor environments (DE), $\vec{\xi}^{\,i}$, for the N-atom system. Which describes most of the interatomic bond energies by a many-body term [12, 21] that are obtained from the atomic density ρ^i between the atoms i and j as [26],

$$\rho^i(\vec{r}) = \sum_{nlm}^{NLM} c_{nlm}^{(i)} g_n(r) Y_{lm}(\hat{r}), \qquad (2)$$

with $Y_{lm}(\hat{r})$ as the spherical harmonics and a set of basis functions in radial directions $g_n(r)$ as $c_{nlm}^{(i)} = \langle g_n Y_{lm} | \rho^i \rangle$ [9, 26]. Thus, the sum over the order m of the squared modulus of the coefficients c_{nlm} that is invariant under rotations around the central atom [27] defines the DE as

$$\vec{\xi}_k^{\,i} = \left\{ \sum_m \left(c_{nlm}^i \right)^* c_{n'lm}^i \right\}_{n,n',l}, \qquad (3)$$

where c_{nlm}^* denotes the complex conjugate of c_{nlm}. In order to perform MD simulations for collisions cascades, the original GAP for W was modified to include a realistic repulsive pair potential, V_{pair}, according to methodology used to develop EAM and Tersoff-like potentials. Here, the smooth connection between the trained GAP and V_{pair} is done by adding dimer distances larger than 1.1 Å in the training database. In addition, several short-range environments are included in the training data set by randomly placing atoms to both perfect crystalline structures and systems containing one or two vacancies; capturing the short-range many-body dynamics in collision cascades for BCC W samples. Finally, it is important to note that the modified GAP becomes numerically unstable at internuclear distance below 0.03 Å which cannot be reached in high-energy cascade simulations.

B. Fingerprinting and Visualization Analyzer of Defects

The machine learning based software workflow FaVAD [20, 22] is applied to the output data of the MD simulations to identify and quantify the number of formed self interstitial atoms (SIAs) and vacancies during collision

cascades. FaVAD describes the local atomic environment of the i-th atom of the damaged material by the normalized DE $\vec{q}\,^i = \vec{\xi}\,^i/|\vec{\xi}\,^i|$ and compares to those for a defect free environment, at a given temperature, to identify the point defects in the damaged material by computing their distance difference as [9, 20].

$$d^M(T) = \sqrt{\left(\vec{q}\,^i - \vec{Q}\,(T)\right)^{\mathrm{T}} \Sigma^{-1}(T) \left(\vec{q}\,^i - \vec{Q}\,(T)\right)}, \quad (4)$$

where $\vec{Q}\,(T) = \frac{1}{N}\sum_{i=1}^{N} \vec{q}\,^i\,(T)$ is the mean of the DEs of the defect free sample; and Σ is the associated co-variance matrix of the DE components [9, 28]. This calculation allows us to quantify point defects at different temperatures, where thermal motion is very important. The identification of vacancies is done by the computation of the nearest neighbor distance between the position of the damaged sample atoms and sampling grid points that defines the spatial volume of the identified vacancy [20, 29].

III. RESULTS AND DISCUSSION

The analysis of the final frame of the MD simulations provides the information of the point defects formed that can be identified and quantified by FaVAD. In Fig. 2, we present results for the comparison between the damage material environment to a defect free one, for different sample temperatures. For the chosen MD simulations, the velocity of the projectile is parallel to the [111] orientation. Note that the thermal motion due to height temperature is observed by the lattice distortion at 0.25 to 0.35 $d^M(T)$. The threshold that defines the actual self interstitial atoms (SIAs) in the sample needs to be assigned according to the sample temperature, where a
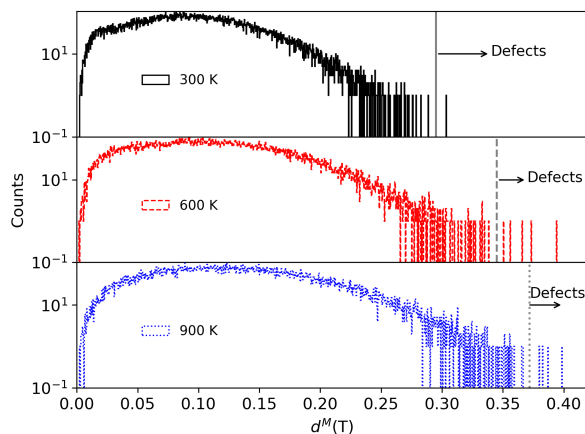

FIG. 2. (Color on-line). Distance difference, $d^M(T)$, between the defect free environment and the W damaged sample at different temperatures. A threshold is defined for each case to identify and quantify points defects by considering the atomic thermal motion.

gap between these defects and atoms in their lattice position is observed for all the cases. FaVAD identified and quantified the production of Frenkel pairs for all the sample where the maximum number of defects is found at 600 K, and decreases at higher temperatures. At a PKA of 1 keV and due to the training data set of the GAP potentials, FaVAD did not find another type of defect. In Tab. I, we report the number of identified and quantified point defects in the damaged material, as reference, and noticing an increase of the Frenkel pair production due to high sample temperature.

In order to investigate the sample temperature effects on the material's damage. We compute the von Mises atomic strain by considering the atomic distance difference, **d**, between the the m-th nearest neighbors of the n-th atom of the pristine and damaged samples as:

$$\boldsymbol{J}_n = \left(\sum_m \boldsymbol{d}_m^{0T}\boldsymbol{d}_m^0\right)^{-1}\left(\sum_m \boldsymbol{d}_m^{0T}\boldsymbol{d}_m\right). \quad (5)$$

Thus, defining the Lagrangian strain matrix of the n-th atom as [30]:

$$\boldsymbol{\eta}_n = 1/2\left(\boldsymbol{J}_n\boldsymbol{J}_n^T - I\right), \quad (6)$$

and the corresponding von Mises strain of the n-th atom is computed as:

$$\eta_n = \sqrt{\frac{\zeta_{ij}\zeta_{ij}}{2}}, \quad \text{with} \quad \zeta_{ij} = \eta_{ij} - \eta_{kk}\delta_{ij}. \quad (7)$$

This approach is implemented in OVITO [31]. In Fig. 3, we report the von Mises strain distribution of the damaged sample at 300 in a), 600 in b), and 900 K in c). Fig. 3 d) shows a histogram of the results comparison, as a reference. Atoms with strain values less than 0.1 are associated to atoms in the BCC lattice point and deleted from the sample for better visualization of the collision cascade. It is observed that the von Mises strain computation provides information of the geometry of the collision cascade, where atoms with a strain from 0.2 to 0.4 are found to be around the formed Frenkel pairs. These atoms are related to the counts maximum of the strain graph shown in Fig 3d). Therefore, the analysis of the damage in W material due to neutron bombardment can be done by quantifying Frenkel pair formed and identifying different defects geometries by FaVAD. In addition,

TABLE I. Average number of point defects and vacancies as a function of the temperature (in Kelvin) identified by FaVAD. SIA are identified as W atoms with the highest probability to be in an interstitial site.

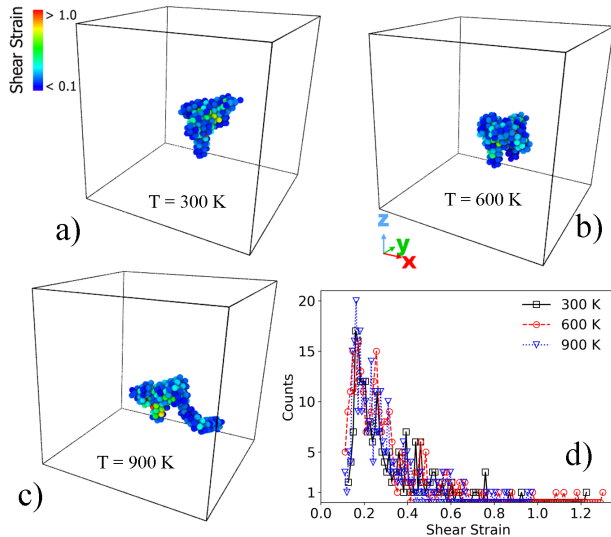| Defect	300	400	600	800	900
SIA	2 ± 1	3 ± 1	5 ± 2	4 ± 1	4 ± 1
NtV.	14 ± 2	18 ± 2	33 ± 5	27 ± 3	25 ± 3
Total	16 ± 2	21 ± 2	38 ± 5	31 ± 3	29 ± 2
Vac.	2 ± 1	3 ± 1	5 ± 2	4 ± 1	4 ± 1

FIG. 3. (Color on-line). von Mises strain distribution for the identified point defects at a sample temperature of 300K in a), 600 K in b), and 900 K in c). A comparison of the results is presented in Fig. d) as a histogram.

the computation of atomic strains gives a visualization of the cluster size and geometry of the collision cascades.

IV. CONCLUDING REMARKS

In this paper, we performed machine learned based molecular dynamics simulations to emulate neutron bombardment on [111] W samples in a temperature range of 300 to 900K. Formation of Frenkel pairs are identified and quantified by the software workflow for fingerprinting and visualizing defects in damaged crystal structures (FaVAD), considering the magnitude of the thermal motion also. At room temperature, the number of Frenkel pair is 2 ± 1 as reported in the literature [16, 32]. The increase of the sample temperature affects the atomic motion in the material and its recovery after collision cascade, producing 4 ± 1 Frenkel pairs at the highest temperature. The computation of the atomic strain is used to visualize the geometry of atoms affected due to collision cascade and the cluster size, where W atoms with a strain between 0.2 and 0.4 are found to be around the formed Frenkel pairs.

[1] Wirth B D, Hu X, Kohnert A and Xu D 2015 *Journal of Materials Research* **30** 1440

[2] Mason D R, Yi X, Sand A E and Dudarev S L 2018 *EPL (Europhysics Letters)* **122** 66001 URL https://doi.org/10.1209/0295-5075/122/66001

[3] Fikar J, Schäublin R, Mason D R and Nguyen-Manh D 2018 *Nuclear Materials and Energy* **16** 60 – 65

[4] Ehrlich K, Bloom E and Kondo T 2000 *Journal of Nuclear Materials* **283-287** 79 – 88 ISSN 0022-3115 9th Int. Conf. on Fusion Reactor Materials URL http://www.sciencedirect.com/science/article/pii/S0022311500001021

[5] Bonny G, Terentyev D, Bakaev A, Grigorev P and Neck D V 2014 *Modelling and Simulation in Materials Science and Engineering* **22** 053001

[6] Herrmann A, Greuner H, Jaksic N, Balder M, Kallenbach A *et al.* 2015 *Nucl. Fusion* **55** 063015

[7] Bolt H, Barabash V, Federici G, Linke J, Loarte A, Roth J and Sato K 2002 *Journal of Nuclear Materials* **307-311** 43 – 52

[8] Marian J, Becquart C S, Domain C, Dudarev S L, Gilbert M R, Kurtz R J, Mason D R, Nordlund K, Sand A E, Snead L L, Suzudo T and Wirth B D 2017 *Nuclear Fusion* **57** 092008

[9] Domínguez-Gutiérrez F and von Toussaint U 2019 *Journal of Nuclear Materials* **528** 151833

[10] Nordlund K 1995 *Computational Materials Science* **3** 448 – 456 ISSN 0927-0256 URL http://www.sciencedirect.com/science/article/pii/092702569400085Q

[11] Nordlund K, Wallenius J and Malerba L 2005 *Nucl. Instr. Meth. Phys. Res. B* **246** 322–332

[12] Byggmästar J, Hamedani A, Nordlund K and Djurabekova F 2019 *Phys. Rev. B* **100** 144105

[13] Nordlund K, Zinkle S J, Sand A E, Granberg F, Averback R S, Stoller R, Suzudo T, Malerba L, Banhart F, Weber W J, Willaime F, Dudarev S and Simeone D 2018 *J. Nucl. Mater.* **512** 450–479

[14] Daw M S and Baskes M I 1984 *Phys. Rev. B* **29**(12) 6443–6453

[15] Rudakov D L, Boedo J A, Moyer R A, Litnovsky A, Philipps V, Wienhold P, Allen S L, Fenstermacher M E, Groth M, Lasnier C J, Boivin R L, Brooks N H, Leonard A W, West W P, Wong C P C, McLean A G, Stangeby P C, De Temmerman G, Wampler W R and Watkins J G 2006 *Review of Scientific Instruments* **77** 10F126

[16] Domínguez-Gutiérrez F, Byggmästar J, Nordlund K, Djurabekova F and von Toussaint U 2020 *Nuclear Materials and Energy* **22** 100724

[17] Bartók A P, Payne M C, Kondor R and Csányi G 2010 *Phys. Rev. Lett.* **104**(13) 136403

[18] Hamedani A, Byggmästar J, Djurabekova F, Alahyarizadeh G, Ghaderi R, Minuchehr A and Nordlund K 2020 *Materials Research Letters* **8** 364–372

[19] Domínguez-Gutiérrez F and Krstić P 2017 *Journal of Nuclear Materials* **492** 56 – 61

[20] von Toussaint U, Domínguez-Gutiérrez F, Compostella M and Rampp M 2021 *Computer Physics Communications* **262** 107816 URL `https://www.sciencedirect.com/science/article/pii/S0010465520304094`

[21] Byggmästar J, Nordlund K and Djurabekova F 2020 *Phys. Rev. Materials* **4**(9) 093802 URL `https://link.aps.org/doi/10.1103/PhysRevMaterials.4.093802`

[22] 2020 `https://gitlab.mpcdf.mpg.de/NMPP/favad/-/tree/master/`

[23] Nordlund K, Zinkle S J, Sand A E, Granberg F, Averback R S, Stoller R, Suzudo T, Malerba L, Banhart F, Weber W J, Willaime F, Dudarev S and Simeone D 2018 *Nature communications* **9** 1084

[24] Plimpton S 1995 *Journal of Computational Physics* **117** 1 – 19

[25] 2018 `http://libatoms.github.io/QUIP/`

[26] Bartók A P, Kondor R and Csányi G 2013 *Phys. Rev. B* **87** 184115

[27] Szlachta W J, Bartók A P and Csányi G 2014 *Phys. Rev. B* **90** 104108

[28] Mahalanobis P 1930 *J. and Proc. Asiat. Soc. of Bengal* **26** 541

[29] von Toussaint U, Dominguez-Gutierrez F, Compostella M and Rampp M 2020 *Computer Physics Communications* 107816 URL `http://www.sciencedirect.com/science/article/pii/S0010465520304094`

[30] Shimizu F, Ogata S and Li J 2007 *Materials Transactions* **48** 2923–2927

[31] Stukowski A 2010 *Modelling and simulation in materials science and engineering* **18** ISSN 0965-0393

[32] Bjoerkas C, Nordlund K and Dudarev S 2009 *Nuclear Instruments and Methods in Physics Research Section B: Beam Interactions with Materials and Atoms* **267** 3204–3208 ISSN 0168-583X proceedings of the Ninth International Conference on Computer Simulation of Radiation Effects in Solids URL `https://www.sciencedirect.com/science/article/pii/S0168583X09007575`